Construction and transmembrane dissociation behavior of supramolecular assembly of quinolinocyclodextrin with porphyrin†

Miao Yu, Yong Chen, Ning Zhang and Yu Liu*

Received 5th May 2010, Accepted 22nd June 2010
First published as an Advance Article on the web 26th July 2010
DOI: 10.1039/c0ob00080a

Through the stoichiometric 2 : 1 coordination of Zn^{2+} with 4-amino-*N*-(2-methylquinolin-8-yl)benzenesulfonamide-modified per-methyl-β-cyclodextrin (MQAS-PMCD) and the strong inclusion complexation of permethyl-β-cyclodextrin cavity with *meso*-tetrakis-(4-sulfonatophenyl)-porphyrin (TSPP), an environment-sensitive Zn^{2+}/cyclodextrin/porphyrin triad supramolecular assembly was constructed, and its structure was fully characterized by UV/vis spectroscopy, fluorescence spectroscopy, powder X-ray diffraction (XRD), scanning tunneling microscopy (STM) and transmission electron microscopy (TEM). Fluorescence spectrometric studies showed that this supramolecular assembly was stable and barely emitted green fluorescence in water due to the energy transfer process, but gave the strong green fluorescence when changing to a hydrophobic environment due to the disruption of the assembly. Further studies on the cell staining experiments by means of fluorescence microscopy showed that this supramolecular assembly was disrupted to release the MQAS-PMCD/Zn^{2+} and porphyrin components when interacting with the cell membrane. Subsequently, the released MQAS-PMCD/Zn^{2+} complex remained in the cell membrane, while the porphyrin component entered the cells. This transmembrane dissociation property of the supramolecular assembly will enable its application in the delivery of biological and drug molecules containing the anionic porphyrin skeleton such as β-octaphenyl-*meso*-tetra(4-carboxyl)-phenylporphyrin and so on.

Introduction

Over the past two decades, designing safe and efficient delivery systems to release their cargo in a controllable manner has been one of the research hot spots for therapeutic delivery systems.[1] Since the environment-sensitive process is very important for biological systems,[2] it has gained increasing interest in the field of designing delivery systems according to physiological needs.[3] In previous reports, polymers have been widely used in therapeutic delivery systems,[4] but the low efficiency limits their applications in clinical trials to a great degree.[5] Recently, supramolecular materials, which are generated *via* the intermolecular non-covalent association of small molecules as building blocks by the "bottom up" approach, have become one fascinating research area for biomedical and pharmaceutical applications. For example, supramolecular materials can serve as models for understanding the self-assembled structures and the molecular recognition in organisms.[6] In addition, supramolecular materials also provide an effective strategy to engineer materials with both the advantages of conventional cross-linked materials and the ability to tailor specific bulk material properties.[7] Among the various molecules used in the construction of supramolecular materials, cyclodextrins (CDs), a class of cyclic oligosaccharides with six to eight D-glucopyranose units linked by α-1,4-glucoside bonds, are extensively studied as not only excellent receptors for molecular recognition but also convenient building blocks to construct nanostructured functional materials,[8] especially bioactive materials and environment-sensitive candidates.[9] On the other hand, anionic porphyrins, such as β-octaphenyl-*meso*-tetra(4-carboxyl)phenylporphyrin,[10] tetra-(carboranyl)-phenyltetrabenzoporphyrin[11] and so on, were widely used as photodynamic therapy (PDT) agents.[12] Moreover, heme-containing proteins, a class of anionic porphyrin/protein system, have very important functions for the oxygen transport and activation in biological processes.[13] Therefore, one can hypothesize that the combination of CD and anionic porphyrin may bring a breakthrough in many fields of biological and medicinal chemistry owing to several inherent advantages. For example, the strong association of the CD cavity, especially the permethyl-β-cyclodextrin (PMCD) cavity with anionic porphyrin,[14] in water can not only prevent the unfavorable porphyrin–porphyrin aggregation,[15] but also enable the high stability of CD/anionic porphyrin system in the biological environments such as body fluid, as well as the transportation of the anionic porphyrin component to the appropriate cellular site without undesirable damage.

Recently, we reported the strong 2 : 1 coordination of 4-amino-*N*-(2-methylquinolin-8-yl)benzenesulfonamide (MQAS)-modified β-CD with Zn^{2+}.[16] Here, we constructed a linear Zn^{2+}/cyclodextrin/porphyrin triad supramolecular assembly through the 2 : 1 coordination of a MQAS-modified PMCD (**1**) with Zn^{2+} and the inclusion complexation of PMCD cavities with *meso*-tetrakis-(4-sulfonatophenyl)-porphyrin zinc complex (ZnTSPP). The structure, morphology and energy transfer properties of the supramolecular assembly were investigated by means

Department of Chemistry, State Key Laboratory of Elemento-Organic Chemistry, Nankai University, Tianjin, 300071, P. R. China. E-mail: yuliu@nankai.edu.cn; Fax: +86-022-23503625; Tel: +86-022-23503625

† Electronic supplementary information (ESI) available: Fluorescence intensity changes, Job's plot, STM image, TG-DTA curves, TG-DTA analysis, and UV/vis spectra. See DOI: 10.1039/c0ob00080a

of UV/vis spectroscopy, fluorescence spectroscopy, powder X-ray diffraction (XRD), scanning tunneling microscopy (STM) and transmission electron microscopy (TEM). Interestingly, the supramolecular assembly showed the environment-sensitive fluorescence behavior due to the controllable association/dissociation between PMCD and ZnTSPP units. More interestingly, the fluorescence spectroscopy and fluorescence microscopy studies of the transmembrane behaviors showed that the ZnTSPP component in this environmental sensitive supramolecular assembly was tightly encapsulated in the PMCD cavity in an aqueous environment but released when entering the cells. This property will consequently meet its potential applications in the delivery of biological or drug molecules containing the anionic porphyrin skeleton.

Results and discussion

Compound **1** was synthesized from 6-amino-permethyl-β-CD and *N*-MQAS-4-amino-4-oxobutanoic acid MQAS-acid in a relatively low yield (<10%) (Scheme 1). A possible reason for the low yield of compound **1** might be the steric hindrance from other methoxyl groups at the 6-positions of the PMCD rim. In addition, the possibility of MQAS-acid forming lactam might be another reason for the low yield. The coordination behavior of **1** with Zn^{2+} was investigated by UV/vis spectroscopy at 25 °C (Fig. 1). With the gradual addition of Zn^{2+}, the UV/vis spectrum of **1** showed a new absorbance peak at 362 nm, and its intensity gradually increased (Fig. 1a). In the control experiment, no appreciable absorbance between 230 and 450 nm could be observed in the UV/vis spectrum of zinc acetate within the appropriate concentration range under the comparable experimental conditions. This UV/vis peak was similar to the characteristic absorbance peaks of several reported five-membered chelate ring structures, which appeared around 360 nm, formed by the coordination of MQAS analogues with Zn^{2+}.[17] Therefore, we deduced that this absorbance band should due to the formation of a five-membered chelate ring between two nitrogen atoms in the MQAS unit of **1** and Zn^{2+}, which extended the conjugated system and thus induced the appearance of a new absorbance band in the long wavelength region. Moreover, the molecular modeling study also demonstrated that the compound **1** could form the stable five-membered chelate ring structure with Zn^{2+} (see the ESI, Figure S7†). Using the UV/vis spectrometry, the coordination stoichiometry between **1** and Zn^{2+} was obtained by the molar ratio method. As seen in Fig. 1b, the curve of $\Delta A_{1/Zn^{2+}}$ ($\Delta A_{1/Zn^{2+}} = A_{1+Zn^{2+}} - A_1$, A_1 was defined as the absorbance intensity of **1** at 362 nm) *vs.* $[Zn^{2+}]/[\mathbf{1}]$ showed an inflexion point at the value of 0.5, which corresponded to a 2 : 1 coordination stoichiometry between **1** and Zn^{2+}. Based on the above observations, the coordination mode of **1**/Zn^{2+} system was shown in Scheme 2.

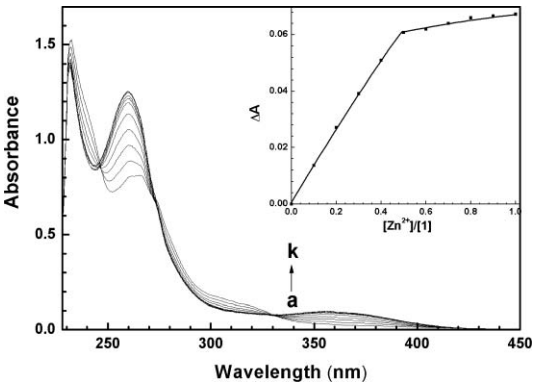

Fig. 1 (a) UV/vis spectra of **1** upon the addition of Zn^{2+} (the counter ion is acetate) in buffer solution (pH 7.20, I = 0.1 mol L^{-1} $NaNO_3$, 25 °C, [**1**] = 50 μmol L^{-1}, $[Zn^{2+}]$ = 0–50 μmol L^{-1} from a to k); (b) The absorbance changes of **1** at 362 nm upon the addition of Zn^{2+}.

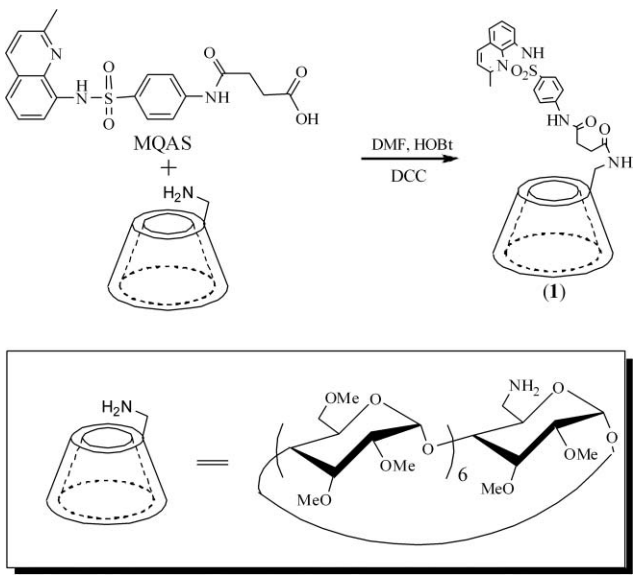

Scheme 1 Synthesis route of MQAS-MCD (**1**).

Using the method of competitive binding,[16] the binding ability of **1** with Zn^{2+} were quantitatively investigated (see the ESI, Figure S1†), and the apparent stability constant (log $K_{1/Zn^{2+}}$, $K_{1/Zn^{2+}} = [Zn{\cdot}\mathbf{1}_2]/[Zn^{2+}][\mathbf{1}]^2$) of $Zn{\cdot}\mathbf{1}_2$ complex was determined as 13.1. Considering the concentrations of **1** and Zn^{2+} employed in the experiments, this strong binding ability of **1** with Zn^{2+} indicated that most of **1** should be converted to $Zn{\cdot}\mathbf{1}_2$ in a stoichiometric 2 : 1 **1**/Zn^{2+} mixture. Therefore, the $Zn{\cdot}\mathbf{1}_2$ complex could be prepared *in situ* by mixing **1** and $Zn(OAc)_2$ with a molar ratio of 2 : 1.

In addition, the binding stoichiometry of **1** with ZnTSPP was also determined by the Job's plot method using UV/vis spectroscopy (see the ESI, Figure S2†).[18] The Job curve showed a maximum at the molar ratio of 0.67, indicating that the formation of a 2 : 1 inclusion complex between **1** and ZnTSPP. This result was consistent with the previous reports about PMCD forming the 2 : 1 inclusion complex with TSPP.[14] The fluorescence titration method gave the binding constant of **1** with ZnTSPP (see the ESI, Figure S3†). According to the 1 : 2 complex stoichiometry, the binding constants K_1 and K_2 could be obtained from the following eqn (1) using the nonlinear least squares curve-fitting method:[19]

$$I = \frac{I_0 + I_1K_1[CD]_0 + I_2K_1K_2[CD]_0^2}{1 + K_1[CD]_0 + K_1K_2[CD]_0^2} \quad (1)$$

Where I was the fluorescence intensity at the given **1** concentration, I_0 was the fluorescence intensity in the absence of **1**, while I_1 and I_2 were the fluorescence intensities of 1 : 1 and 1 : 2 complexes, respectively.

By monitoring the fluorescence intensity changes at 652 nm, the values of log K_1 and log K_2 between **1** and ZnTSPP were obtained

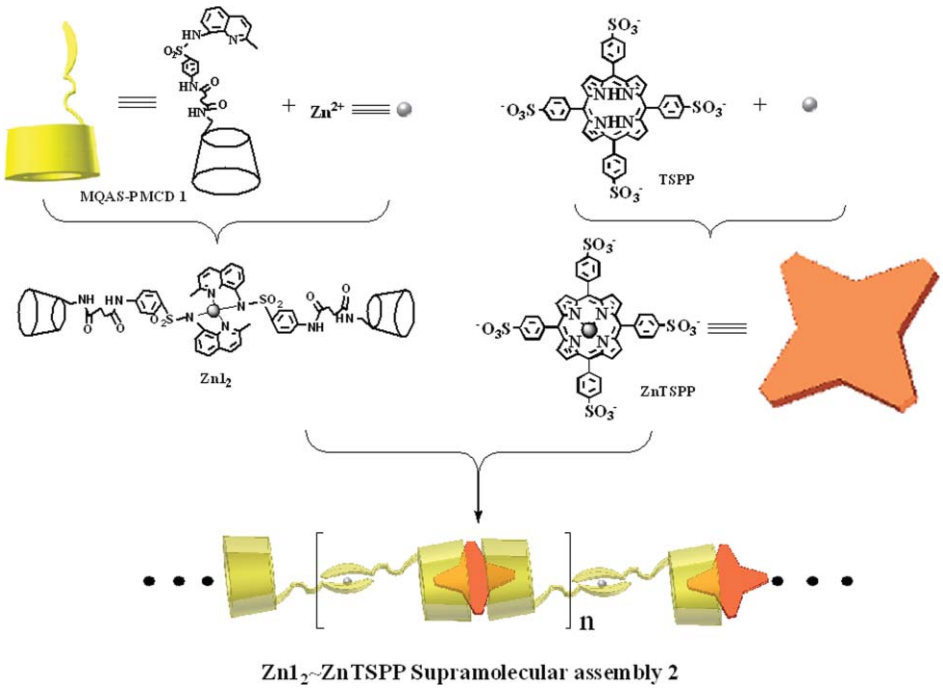

Scheme 2 Preparation route of supramolecular assembly **2**.

as 4.60 ± 0.17 and 5.60 ± 0.42 respectively (see the ESI, Figure S3†).

Owing to the strong association of Zn·**1**$_2$ (log $K_{\mathbf{1}/Zn^{2+}}$ = 13.1) and **1**/ZnTSPP (log $K_{\mathbf{1}/ZnTSPP}$ = log $K_1 \cdot K_2 > 9$) systems in aqueous solution, we deduced that Zn·**1**$_2$–ZnTSPP supramolecular assembly **2** could be constituted *in situ* in a Zn^{2+}/**1**/ZnTSPP (molar ratio = 1 : 2 : 1) solution through a cooperative contribution of the metal coordination of Zn^{2+} with **1** and the host–guest association of ZnTSPP with **1**. The possible structure of **2** is shown in Scheme 2.

The microstructure of supramolecular assembly **2** was investigated by XRD, because the XRD patterns of a sample could reflect the statistically microstructures characters in it.[20] As seen in Fig. 2, the microstructure of Zn·**1**$_2$ was somewhat amorphous (Fig. 2b), but the sharp peaks over the diffraction angles indicated the crystal nature of ZnTSPP (Fig. 2a). In the control experiment, the XRD pattern (Fig. 2c) of the physical mixture of Zn·**1**$_2$ with ZnTSPP showed a diffractogram that could be characterized as a superimposition of Zn·**1**$_2$'s and ZnTSPP's diffractograms. In contrast, the XRD pattern of **2** exhibited the appreciable differences from that of the physical mixture in terms of the peak shape, peak position and relative intensity. In the XRD of **2** (Fig. 2d), the intensity of the diffraction peaks decreased, while its width increased, as compared with those of the physical mixtures, accompanied by the disappearance of several characteristic peaks (2θ = 4.8, 5.68 and 7.78°) of ZnTSPP. These phenomena indicated that the new species between Zn·**1**$_2$ and ZnTSPP was formed in the solid state, and the original arrangement mode of ZnTSPP was changed after the introduction of Zn·**1**$_2$.

Other information about the microstructure of assembly **2** came from the transmission electron microscopy (TEM) and scanning tunneling microscopy (STM). As seen in Fig. 3, the TEM image of **2** showed a few one-dimensional linear structures with an average width of 2–3 nm[21] and an approximate length of 50–60 nm. At the same time, STM images (see the ESI, Figure S4†) also demonstrated similar characteristics for **2**. Through the terminal group analysis using the data of TG-DTA, we also obtained the molecular weight of assembly **2** (see the ESI, Figure S5†) as *ca.* 2.3 × 10^5 g mol^{-1}. These results jointly indicated the formation of a highly-ordered supramolecular array in solution.

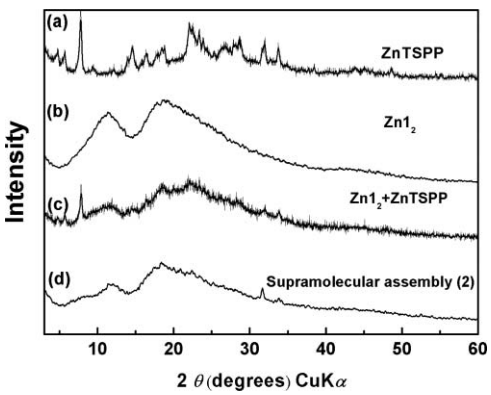

Fig. 2 XRD patterns of (a) ZnTSPP, (b) Zn·**1**$_2$, (c) physical mixture of Zn·**1**$_2$ with ZnTSPP, and (d) supramolecular assembly **2**.

Interestingly, the association with ZnTSPP greatly quenched the fluorescence of Zn·**1**$_2$. As seen in Fig. 4, the fluorescence of Zn·**1**$_2$ decreased with the stepwise addition of ZnTSPP. When the molar ratio of Zn·**1**$_2$ *vs.* ZnTSPP reached 1 : 1, the fluorescence emission of Zn·**1**$_2$ at 500 nm was completely quenched. To explore the possible fluorescence quenching mechanism of Zn·**1**$_2$ upon the addition of ZnTSPP, some control experiments were carried out. We noticed that the Q-band (450–580 nm) of ZnTSPP ground state (see the ESI, Figure S6†) was overlapped with the emission band of Zn·**1**$_2$ (400–630 nm). In the steady fluorescence experiment,

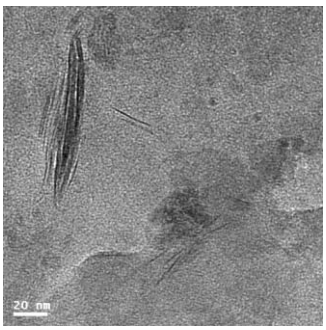

Fig. 3 TEM micrograph of sample of assembly **2**.

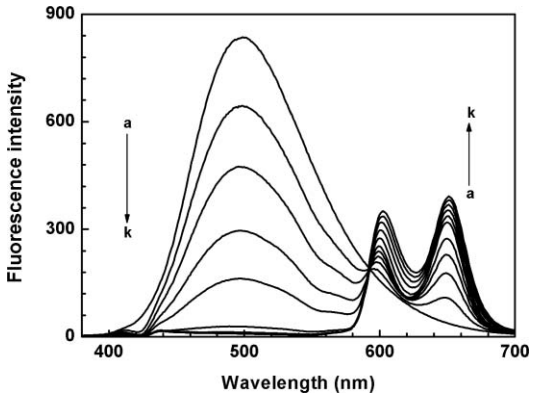

Fig. 4 Fluorescence spectral changes of Zn·$\mathbf{1}_2$ (10 μmol L^{-1}) with the addition of ZnTSPP ([ZnTSPP] = 2–20 μmol L^{-1} from lines a to k) in buffer solution (pH 7.20, I = 0.1 mol L^{-1} $NaNO_3$, 25 °C, λ_{ex} = 362 nm).

the fluorescence intensity of ZnTSPP at 650 nm increased with the addition of Zn·$\mathbf{1}_2$ even after taking account into the effect of PMCD cavity (Fig. 5). On the basis of these observations, we deduced that the fluorescence quenching of Zn·$\mathbf{1}_2$ by ZnTSPP might be due to an energy transfer process,[22] that is, the energy was transferred from the electronically excited state of Zn·$\mathbf{1}_2$ (donor) to the ground-state of ZnTSPP (acceptor).

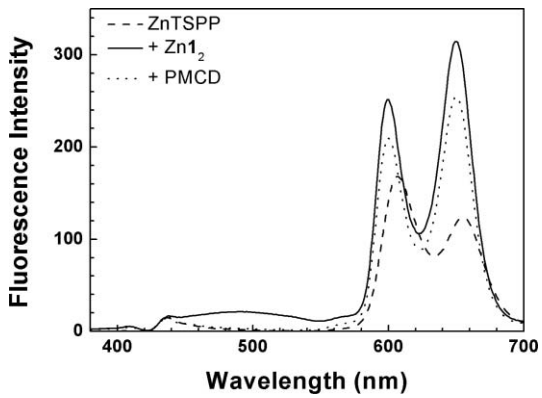

Fig. 5 Fluorescence spectra of ZnTSPP (10 μmol L^{-1}, the dash line), and in the presence of Zn·$\mathbf{1}_2$ (10 μmol L^{-1}, the solid line) or PMCD (20 μmol L^{-1}, the dot line) in aqueous buffer solution (pH 7.20, I = 0.1 mol L^{-1} $NaNO_3$, 25 °C, λ_{ex} = 362 nm).

The acceptor released from its steric proximity to the donor would lead to the abolishment of energy transfer process and the activation of donor fluorophore. Therefore, a fluorescence recovery experiment was also performed. With increasing portion of EG in solvent, the fluorescence of Zn·$\mathbf{1}_2$/ZnTSPP system gradually recovered, and the fluorescence intensity changes of Zn·$\mathbf{1}_2$ at 500 nm were negligible with the addition of ZnTSPP in the pure EG solution under the same conditions. A possible reason for the fluorescence recover might be as follow. Increasing the portion of EG increased the hydrophobicity of the solvent, which consequently led to the release of ZnTSPP from the PMCD cavity of **1**. As a result, the energy transfer process was abolished. Significantly, the release of ZnTSPP also resulted in the dissociation of the assembly **2**. This controllable dissociation behavior of assembly **2** with the environmental change would enable its application potential as an environment-sensitive delivery system.

A preliminary study on the application of the controllable dissociation of **2** in the biological system was performed by fluorescence spectroscopy and fluorescence microscopy. Herein, the lecithin liposome lamellar vesicle was used as models to mimic the lipid layers of cells.[23] As seen in Fig. 6, the fluorescence intensity of **2** at ~500 nm increased remarkably in the presence of lecithin liposome (2 g dm^{-3}). This phenomenon may be ascribed to the penetration of **2** into the liposome vesicle, which increased the microenvironmental hydrophobicity around **2**. The transfer of **2** from polar water phase to apolar hydrophobic environment, such as the hydrocarbon core of lecithin liposome vesicle, led to the release of ZnTSPP from the PMCD cavity of **1** and thus resulted in the enhanced fluorescence of Zn·$\mathbf{1}_2$. This result indicated that the assembly **2** had a possibility of dissociation when interacting with the cell membrane.

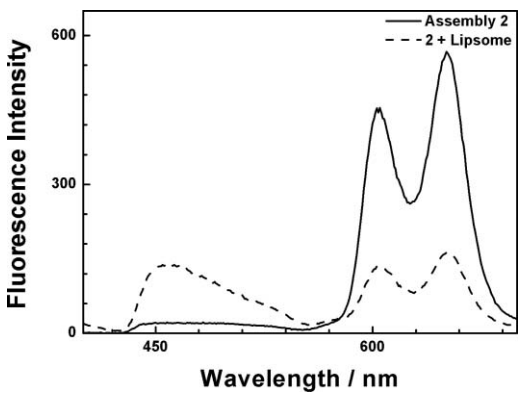

Fig. 6 Fluorescence spectral changes of **2** (10 μmol L^{-1}, the solid line) with the addition of lecithin liposome (2 g dm^{-3}, the dash line) in aqueous buffer solution (pH 7.2, I = 0.1 mol L^{-1} $NaNO_3$, 25 °C, λ_{ex} = 362 nm).

Possessing many analogous features to mammalian cells, yeast cells were used as the substrate in cell staining studies. In our experiments, the pre-cultured yeast cells were transferred to a solution of Zn·$\mathbf{1}_2$, ZnTSPP or assembly **2**, and the fluorescence microscopic images were performed after incubation for *ca.* 3 h. As seen in Fig. 7, the yeast cells treated by Zn·$\mathbf{1}_2$ emitted the fairly weak green fluorescence when excited at 362 nm (Fig. 7b) and presented no fluorescence when excited at 556 nm (Fig. 7c), while the cells treated by ZnTSPP emitted the weak red fluorescence when excited at 362 nm (Fig. 7e) and a little stronger red fluorescence when excited at 556 nm (Fig. 7f). This phenomenon indicated that ZnTSPP had a limited, while Zn·$\mathbf{1}_2$ poor, ability of interacting with the cells. However, when treated by the assembly

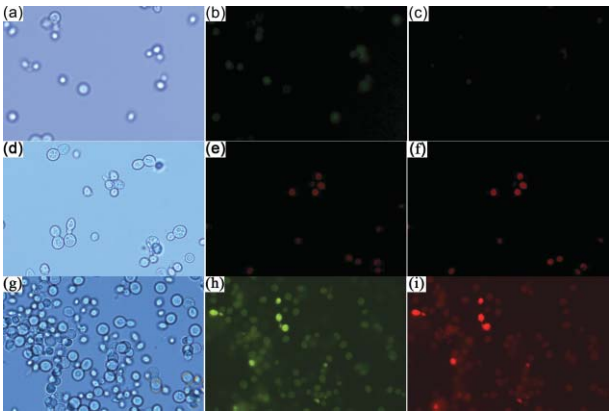

Fig. 7 The optical microscopic images (a, d, g) and fluorescence microscopic images (b, c, e, f, h, i) of yeast cells stained with Zn·**1**$_2$ (20 μmol L^{-1}), ZnTSPP (20 μmol L^{-1}), assembly **2** (0.1 g L^{-1}, *i.e.* 20 μmol L^{-1} calculated as the concentration of Zn·**1**$_2$ or ZnTSPP component) in aqueous solution. The fluorescence microscopic images were excited at 362 nm (b, e, h) and 556 nm (c, f, i).

2, the cells emitted bright green fluorescence when excited at 362 nm (Fig. 7h). As described above, the assembly **2** could not emit green fluorescence due to the energy transfer process. Therefore, the green fluorescence of the **2**-stained cells should be attributed to the emission of free Zn·**1**$_2$. In addition, when excited at 556 nm, the **2**-stained cells also emitted the red fluorescence, like the case of the ZnTSPP-stained cells. A possible reason of these phenomena should be as follow. The binding ability between the cavity of PMCD and ZnTSPP could decrease even to 0 with the environmental hydrophobicity increasing.[14] Therefore, when the assembly **2** entered the hydrophobic environment of lipid layers of cells, the binding ability between PMCD cavity and ZnTSPP greatly decreased, which led to the disruption of the assembly, and then the PMCD cavity bound the cholesterol in the cell membrane due to the stronger binding ability between cholesterol and the PMCD cavity.[24] The interaction with the cell membrane led to the disruption of assembly **2**, and, as a result, Zn·**1**$_2$ and ZnTSPP were released. Andrews and co-workers reported that[25] 6-methoxy-(8-*p*-toluenesulfonamido)-quinoline (TSQ), an analogue with a high structural similarity to the MQAS moiety of **1**, and its Zn^{2+} complex had high affinities towards the phosphatidylcholine membrane, and TSQ still remained in the membrane after the complexation with Zn^{2+}. Therefore, we deduced that Zn·**1**$_2$ released from the assembly **2** should settle in the cell membrane and thus emit the green fluorescence when excited at 362 nm. On the other hand, ZnTSPP released from the assembly **2** should enter the cells, like the widely reported results that the anionic porphyrins were able to enter the cells,[10–12] and emit red fluorescence when excited at 556 nm. Considering the stronger red fluorescence of the **2**-stained cells (*ca.* 2.5 times) than that of the ZnTSPP-stained ones when excited at 556 nm, we deduced that the efficiency of delivering ZnTSPP into the cells by **2** was fairly higher than that of the free ZnTSPP, although the possibility of some **2** entering the cells as a whole could not be rigorously ruled out.

Conclusions

A Zn^{2+}/cyclodextrin/porphyrin triad supramolecular assembly has been successfully constructed through a cooperative contribution of the host–guest inclusion complexation and the metal coordination. In aqueous solution, this supramolecular assembly was stable due to the strong binding between the PMCD cavity of **1** and the anionic porphyrin. When changing to a hydrophobic environment, such as the cell membrane, this supramolecular assembly would be disrupted to release the porphyrin components into the cells. This environment-sensitive property, along with the easy preparation, would enable the potential application of the supramolecular assembly as the drug delivery carriers, especially in the delivery of biological and drug molecules containing the anionic porphyrin skeletons.

Experimental

General methods

All chemicals used in this report were reagent grade unless noted. 2-Methyl-8-amino-quinoline was obtained from J & K Chemical LTD. *Meso*-tetrakis-(4-sulfonatophenyl)-porphyrin tetrasodium salt (TSPP) was obtained from Sigma-Aldrich Co. Acetanilide, chlorosulfuric acid, and succinic anhydride were all obtained from Aldrich. Tris-HCl buffer solution (pH 7.2) was used as solvent in all spectral measurements without specially mentioned. 6^{I}-Amino-6^{I}-deoxy-2^{I},3^{I}-di-*O*-methyl-hexakis(2$^{II\text{-}VII}$,3$^{II\text{-}VII}$,6$^{II\text{-}VII}$-tri-*O*-methyl)-*β*-cyclodextrin (6-amino-permethyl-β-CD)[26] and MQAS-acid[16] were prepared according to the reported procedures. *N*,*N*′-Dimethylformamide (DMF) was dried over CaH_2 for 2–3 d and then distilled under reduced pressure at 45 °C prior to use. Lecithin liposome was prepared according to the reported method.[23] The yeast (*Saccharomyces cerevisia*) was obtained as a gift from the Department of Agronomy-Forestry Science, Huanghuai University. Elemental analyses were performed on a Perkin-Elmer-2400C instrument. NMR spectra were recorded on a Bruker 300 spectrometer. UV/vis spectra were recorded in a conventional quartz cell (light path 10 mm) on a Shimadzu UV-2401PC spectrophotometer equipped with a PTC-348WI temperature controller to keep the temperature at 25 °C. Fluorescence spectra were recorded in a conventional quartz cell (10 × 10 × 45 mm) at 25 °C on a Varian Cary eclipse fluorescence spectrometer (xenon lamp photosource) equipped with a single cell Peltier temperature controller accessory to keep the temperature at 25 °C. FT-IR spectra were obtained in KBr pellets with a Bruker Tensor 27 FT-IR. Thermogravimetric (TG) and differential thermal analysis (DTA) were recorded with a Rigaku Standard TG-DTA type. Samples were heated at 10 °C min^{-1} from room temperature to 800 °C in a dynamic nitrogen atmosphere (flow rate = 70 mL min^{-1}). The powder X-ray diffraction (XRD) scans of samples was carried out on a Rigaku D/max-2500 diffractometer. The X-ray source was Ni-filtered Cu-Kα radiation (40 kV, 100 mA). The specimens were mounted on aluminium frames and scanned from 3 to 60° = 2θ at a speed of 2θ = 1.2° min^{-1}. The transmission electron microscopy (TEM) images were recorded by a Philips Tacnai G^2 20 S-TWIN microscope. The sample was obtained from an aqueous solution of sample (1 mmol L^{-1}) with a carbon-coated copper grid. The grid was dried under reduced pressure for 2 h at room temperature. The accelerating voltage of the transmission electron microscope was 200 kV. STM experiments were performed with a Nanosurf instrument (Switzerland) with a Pt–Ir tip at a sample bias voltage

of +300 mV. All images were acquired in constant-current mode. An aqueous solution of assembly (1×10^{-5} mol L^{-1}) was dripped onto a freshly prepared highly ordered pyrolytic graphite (HOPG) surface at RT. The sample was then dried *in vacuo* at 25 °C for 2 h. All measures were performed in air at RT. All optical and fluorescence microscopic images were performed on an OLYMPUS BX51 fluorescence microscope with a 100 W/DC mercury lamp for excitation and a Mc MP5 color CCD camera for photo collection.

Preparation of MQAS-modified permethyl-β-CD (1)

To 40 mL of anhydrate DMF was added MQAS-acid (413 mg, 1 mmol) and 1-hydroxybenzotriazole (HOBt, 200 mg, 1.48 mmol). After the mixture was cooled to 0 °C, *N*,*N*′-dicyclohexylcarbodimide (DCC, 305 mg, 1.48 mmol) was added into the solution. After the mixture was stirred for 2 h at 0 °C, 6-amino-permethyl-β-CD (1.42 g, 1 mmol) was added to the mixture, stirred for 3 h at 0 °C, then at RT for 40 h. The precipitate was removed by filtration. Then the filtrate was concentrated under reduced pressure to obtain the crude product as a yellow solid. The solid was dissolved in CH_2Cl_2. After removing the insoluble matters by filtration, the crude product was purified by chromatography on silica with a gradient elution profile (50 : 1 to 20 : 1, CH_2Cl_2–MeOH) to give the pure product as a pale yellow solid, (150 mg, 8.3% yield). MS (ESI): *m/z* 1809.6 ($[M+H]^+$), 1826.4 ($[M+NH_4]^+$), 1831.7 ($[M+Na]^+$), 1910.4 ($[M+Na+Pyridine]^+$); (1808.8 calcd for $C_{82}H_{128}N_4O_{38}S$); ^{1}H NMR (D_2O, 300 MHz, TMS, ppm): δ 2.64 (s, 4H, CH_2), 2.86 (s, 3H, Quinoline-CH_3), 2.92–4.29 (m, 96H, H2–H4, H6 and CH_3 of PMCD), 4.62 (6H, H5 of PMCD), 5.18 (d, J = 24.6 Hz, 7H, H1 of PMCD), 7.06 (d, J = 7.5 Hz, 1H, Quinoline), 7.39 (s, 1H, Quinoline), 7.49 (s, 2H, Quinoline), 7.62 (s, 1H, Quinoline), 7.74 (d, J = 7.8 Hz, 2H, Ph), 8.10 (d, J = 7.9 Hz, 2H, Ph). Anal. Calcd (%) for $C_{82}H_{128}N_4O_{38}S{\cdot}3H_2O$: C 52.84, H 7.25, N 3.01; Found: C 52.91, H 7.21, N 2.96.

Preparation of metal complex Zn·$\mathbf{1}_2$

Compound **1** (37 mg, 20 μmol) and zinc acetate dihydrate (2.6 mg, 12 μmol) were dissolved in chloroform (12 mL) with stirring at room temperature for 1 h, then incubated for 1 d at 80 °C to obtain the Zn·$\mathbf{1}_2$ solution. And then the solution was removed to obtain the crude metal complex Zn·$\mathbf{1}_2$. The crude product was purified through the G-25 column and dried *in vacuo* to give the pure product as a yellow solid (30 mg, 75% yield). MS (MALDI-TOF): *m/z* 3704.8 ($[M+Na]^+$). ^{1}H NMR (D_2O) for complex was same to the compound **1**. IR(film) 3564, 2963, 2930, 2834, 1679, 1675, 1595, 1538, 1459, 1403, 1333, 1262, 1093, 1033, 970, 894, 802, 753, 703, 570 cm^{-1}; Anal. Calcd (%) for $C_{164}H_{254}N_8O_{76}S_2^{2-}{\cdot}Zn^{2+}{\cdot}H_2O$: C 53.22, H 6.97, N 3.03; Found: C 53.21, H 7.11, N 2.93.

Preparation of assembly 2

To an aqueous zinc acetate dihydrate (1.1 mg, 5 μmol) solution (2 ml), TSPP tetra-sodium salt (5.1 mg, 5 μmol) was added, and the mixture was stirred for 3 h and then incubated for 1 d at RT to obtain the aqueous ZnTSPP solution. Then, Zn·$\mathbf{1}_2$ (20 mg) was added to the aqueous ZnTSPP solution, and the mixture was stirred for 3 h and incubated for 1 d at RT. The mixture was dried under reduced pressure to obtain the crude assembly **2**. The crude product was purified through the G-25 column and dried *in vacuo* to give the pure assembly **2** as a rosy solid (15 mg, 63% yield). ^{1}H NMR (D_2O, 300 MHz, TMS, ppm): δ 1.03–3.96 (218H, H2–H6 and CH_3 of PMCD and Quinoline-CH_3 and –CH_2–CH_2–), 4.92 (14H, PMCD), 6.94 (2H, of Quinoline), 7.29–8.29 (28H, Quinoline and Phenyl of TSPP outside the cavity of PMCD), 8.39 (4H, Phenyl of TSPP inside the cavity of PMCD), 8.84 (4H, pyrrole ring of TSPP), 9.00 (4H, pyrrole ring of TSPP). Anal. Calcd (%) for $C_{208}H_{282}N_{12}O_{88}S_6^{4-}{\cdot}14H_2O{\cdot}2Zn^{2+}$: C 50.03, H 6.18, N 3.37; Found: C 49.96, H 6.22, N 3.43.

Preparation of yeast cell stain sample

The yeast (*Saccharomyces cerevisia*) cell sample was dispersed in the media of YPD (2.0% yeast extract, 4% peptone, 2.0% glucose, 0.2% $(NH_4)_2SO_4$) and then cultured for 3 d at 35 °C. The obtained aqueous colonies solutions, which were selected for cell staining, were incubated in the dark for 3 h at 35 °C with Zn·$\mathbf{1}_2$ (20 μmol L^{-1}), ZnTSPP (20 μmol L^{-1}) or assembly **2** (0.1 g L^{-1} *i.e.* 20 μmol L^{-1} calculated as the concentration of Zn·$\mathbf{1}_2$ or ZnTSPP component), respectively. Subsequently, these stained cells were collected by centrifugation to remove the uncombined stain agent. The stained yeast cells were dispersed in distilled water for further experiments.

Acknowledgements

We thank 973 Program (2006CB932900), NNSFC (20932004, 20721062 and 20772062), Tianjin Natural Science Foundation (07QTPTJC29600) for financial support.

Notes and references

1 K. Uekama, F. Hirayama and T. Irie, *Chem. Rev.*, 1998, **98**, 2045; B. G. Trewyn, S. Giri, I. I. Slowing and V. S.-Y. Lin, *Chem. Commun.*, 2007, 3236.
2 Y. Bae, S. Fukushima, A. Harada and K. Kataoka, *Angew. Chem., Int. Ed.*, 2003, **42**, 4640.
3 P. Bawa, V. Pillay, Y. E. Choonara and L. C. du Toit, *Biomed. Mater.*, 2009, **4**, 022001; M. P. Lutolf and A. Hubbell, *Nat. Biotechnol.*, 2005, **23**, 47.
4 R. Kumar, M.-H. Chen, V. S. Parmar, L. A. Samuelson, J. Kumar, R. Nicolosi, S. Yoganathan and A. C. Watterson, *J. Am. Chem. Soc.*, 2004, **126**, 10640; K. C. Wood, S. R. Little, R. Langer and P. T. Hammond, *Angew. Chem., Int. Ed.*, 2005, **44**, 6704.
5 R. Kircheis, L. Wightman and E. Wagner, *Adv. Drug Delivery Rev.*, 2001, **53**, 341.
6 J. M. Lehn, *Science*, 1993, **260**, 1762; G. M. Whitesides and B. Grzybowski, *Science*, 2002, **295**, 2418.
7 M. C. Branco and J. P. Schneider, *Acta Biomater.*, 2009, **5**, 817; L. Brunsveld, B. J. B. Folmer, E. W. Meijer and R. P. Sijbesma, *Chem. Rev.*, 2001, **101**, 4071; D. K. Smith, *J. Chem. Educ.*, 2005, **82**, 393; V. J. Stella and R. A. Rajewski, *Pharm. Res.*, 1997, **14**, 556.
8 G. Wenz, B-H. Han and A. Müller, *Chem. Rev.*, 2006, **106**, 782; H. Yamaguchi, T. Oshikiri and A. Harada, *J. Phys.: Condens. Matter*, 2006, **18**, S1809; D. Armspach, P. R. Ashton, C. P. Moore, N. Spencer, J. F. Stoddart, T. J. Wear and D. J. Williams, *Angew. Chem., Int. Ed. Engl.*, 1993, **32**, 854; A. Harada, *Acc. Chem. Res.*, 2001, **34**, 456; Y. Liu and Y. Chen, *Acc. Chem. Res.*, 2006, **39**, 681; Y. Chen and Y. Liu, *Chem. Soc. Rev.*, 2010, **39**, 495.
9 L. Zhu, D. Zhang, D. Qu, Q. Wang, X. Ma and H. Tian, *Chem. Commun.*, 2010, **46**, 2587; R. Alvarez-Rodríguez, F. J. Arias, M. Santos, A. M. Testera and J. C. Rodríguez-Cabello, *Macromol. Rapid Commun.*, 2010, **31**, 568; X. Liao, G. Chen, X. Liu, W. Chen, F. Chen and M. Jiang, *Angew. Chem., Int. Ed.*, 2010, **49**, 4409; J. Li and X. J. Loh, *Adv. Drug Delivery Rev.*, 2008, **60**, 1000; M. E. Brewster and T. Loftssona, *Adv. Drug Delivery Rev.*, 2007, **59**, 645.

10 B. Zhai, L. Shuai, L. Yang, X. Weng, L. Wu, S. Wang, T. Tian, X. Wu, X. Zhou and C. Zheng, *Bioconjugate Chem.*, 2008, **19**, 1535.
11 V. Gottumukkala, O. Ongayi, D. G. Baker, L. G. Lomax and M. G. H. Vicente, *Bioorg. Med. Chem.*, 2006, **14**, 1871.
12 J. P. Celli, B. Q. Spring, I. Rizvi, C. L. Evans, K. S. Samkoe, S. Verma, B. W. Pogue and T. Hasan, *Chem. Rev.*, 2010, **110**, 2795.
13 C. Taillé, J. El-Benna, S. Lanone, M-C. Dang, E. Ogier-Denis, M. Aubier and J. Boczkowski, *J. Biol. Chem.*, 2004, **279**, 28681.
14 Y. Liu, C.-F. Ke, H.-Y. Zhang, J. Cui and F. Ding, *J. Am. Chem. Soc.*, 2008, **130**, 600; K. Kano, R. Nishiyabu, T. Asada and Y. Kuroda, *J. Am. Chem. Soc.*, 2002, **124**, 9937.
15 T. Konishi, A. Ikeda, M. Asai, T. Hatano, S. Shinkai, M. Fujitsuka, O. Ito, Y. Tsuchiya and J. Kikuchi, *J. Phys. Chem. B*, 2003, **107**, 11261.
16 Y. Liu, M. Yu, Y. Chen and N. Zhang, *Bioorg. Med. Chem.*, 2009, **17**, 3887.
17 C. J. Fahrni and T. V. O'Halloran, *J. Am. Chem. Soc.*, 1999, **121**, 11448; Y. Liu, N. Zhang, Y. Chen and L.-H. Wang, *Org. Lett.*, 2007, **9**, 315; R. Kataky and M. A. Knell, *J. Solution Chem.*, 2009, **38**, 1483.
18 K. A. Connors *Binding constants*, Wiley, New York, 1987.
19 Y. Inoue, T. Hakushi, Y. Liu, L.-H. Tong, B.-J. Shen and D.-S. Jin, *J. Am. Chem. Soc.*, 1993, **115**, 475; S. Nigam and G. Durocher, *J. Phys. Chem.*, 1996, **100**, 7135.
20 Y. Liu, H. Wang, Y. Chen, C.-F. Ke and M. Liu, *J. Am. Chem. Soc.*, 2005, **127**, 657.
21 J. Shi, D.-S. Guo, F. Ding and Y. Liu, *Eur. J. Org. Chem.*, 2009, 923.
22 J. R. Lakowicz *Principles of Fluorescenc Spectroscopy*, 3nd ed Singapore: Springer2006; K. Kano, R. Nishiyabu, Yamazaki T. and I. Yamazaki, *J. Am. Chem. Soc.*, 2003, **125**, 10625.
23 K. Edwards, M. Johnsson, G. Karlsson and M. Silvander, *Biophys. J.*, 1997, **73**, 258.
24 T. Giesemann, T. Jank, R. Gerhard, E. Maier, I. Just, R. Benz and K. Aktories, *J. Biol. Chem.*, 2006, **281**, 10808.
25 J. C. Andrews, J. P. Nolan, R. H. Hammerstedt and B. D. Bavister, *Biol. Reprod.*, 1994, **51**, 1238.
26 C. Hocquelet, J. Blu, C. K. Jankowski, S. Arseneau, D. Buisson and L. Mauclaire, *Tetrahedron*, 2006, **62**, 11963; I. W. Muderawan, T. T. Ong, Lee T. C., D. J. Young, C. B. Ching and S. C. Ng, *Tetrahedron Lett.*, 2005, **46**, 7905.

